

Addressing overfitting in spectral clustering via a non-parametric bootstrap

Liam Welsh^{*,†}

Phillip Shreeves^{‡,†}

University of Toronto

Simon Fraser University

September 14, 2022

Abstract

Finite mixture modelling is a popular method in the field of clustering and is beneficial largely due to its soft cluster membership probabilities. However, the most common algorithm for fitting finite mixture models, the EM algorithm, falls victim to a number of issues. We address these issues that plague clustering using finite mixture models, including convergence to solutions corresponding to local maxima and algorithm speed concerns in high dimensional cases. This is done by developing two novel algorithms that incorporate a spectral decomposition of the data matrix and a non-parametric bootstrap sampling scheme. Simulations show the validity of our algorithms and demonstrate not only their flexibility but also their ability to avoid solutions corresponding to local-maxima, when compared to other (bootstrapped) clustering algorithms for estimating finite mixture models. Our novel algorithms have a typically more consistent convergence criteria as well as a significant increase in speed over other bootstrapped algorithms that fit finite mixture models.

Keywords: Spectral Clustering, EM Algorithm, Bootstrapping, Dimensionality Reduction, Mixture Models

*Corresponding Author: liam.welsh@mail.utoronto.ca, Department of Statistical Sciences, 9th Floor 700 University Ave., Toronto, ON M5G 1Z5

[†]Authors contributed equally

[‡]Department of Statistics and Actuarial Science

1 Introduction

As the world becomes more saturated with big data, the ability to produce statistical models from high dimensional data is a task of great significance. In the field of clustering, unsupervised learning algorithms are used to find patterns or groups within the underlying untagged data and are able to construct models in high dimensional settings (see [Bouveyron and Brunet-Saumard \(2014\)](#); [Celebi and Aydin \(2016\)](#)). A main issue with constructing such models in these settings is that for data sets with a large amount of predictors, the fitting of these models and parameter estimations can be incredibly slow, converge to local solutions, or lack interpretation. While there exist many choices for dimensionality reduction techniques, such as principal component analysis and various data decomposition methods, the use of these risks losing a non-trivial proportion of the variance in the original data. Further, many clustering algorithms are fraught with issues in both low and high dimensional settings, such as converging to local maxima solutions or overfitting to the data available. [Andrews \(2018\)](#) has demonstrated and addressed the issue of overfitting in finite mixture models (FMMs), however fitting a FMM in a high dimensional setting is computationally non-trivial, as it requires repeated inversions of $p \times p$ covariance matrices with p equal to the number of predictors. FMMs are of particular interest as they provide a probabilistic result for group memberships, allowing for valuable insight into analysis and model interpretation; see [McLachlan et al. \(2019\)](#). To address the issues with overfitting in high dimensional FMMs, we propose the combination of a common dimensionality reduction clustering algorithm called spectral clustering with a non-parametric bootstrap. Spectral clustering is a versatile clustering technique that is useful for high dimensional settings; see [Vempala and Wang \(2004\)](#) and [Von Luxburg \(2007\)](#). However, it is prone to various issues, including overfitting and converging to local maxima, which we address in this paper via a bootstrap augmented approach.

We develop two novel algorithms and show that our proposed algorithms not only address the issue of overfitting, but are also significantly faster than the current bootstrapped approaches. The remainder of this paper is organized as follows. A motivating example is introduced in Section 2. Section 3 follows with the necessary background information required to understand the novel developments in methodology that are presented in Section 4. This includes two bootstrap-augmented algorithms for spectral clustering, as well as an updated form of convergence criteria. Next, the algorithms are analyzed using simulated and real-world data sets Section 5. Concluding remarks are provided in Section 6.

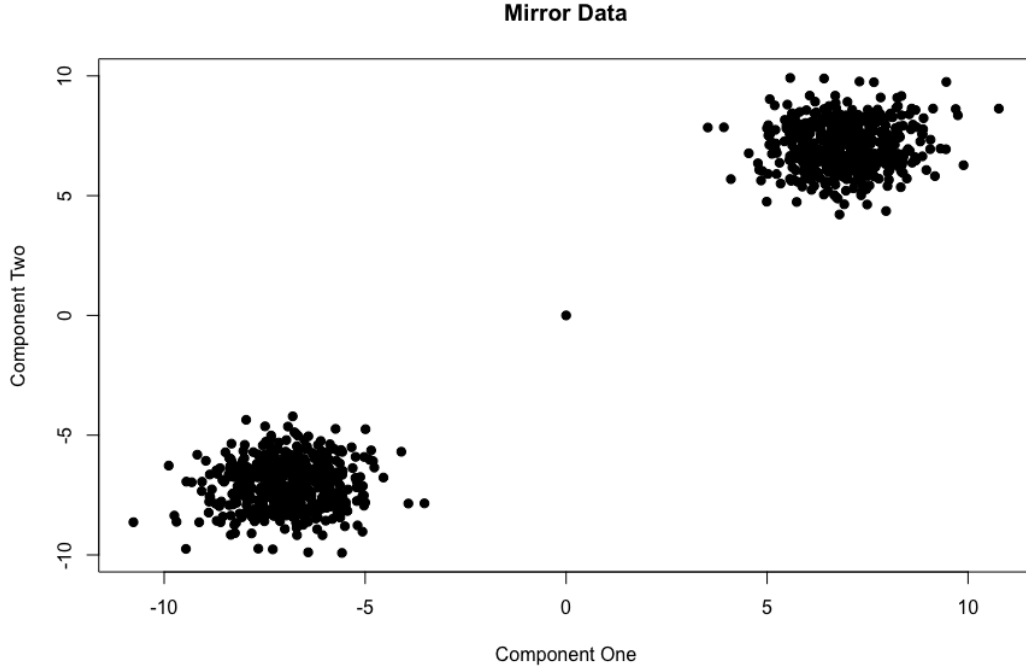


Figure 1: The first two components of a high-dimensional mirror data set. Each pairwise set of components retains the same structure, with group means at $(-7, -7)$ and $(7, 7)$ and a single point at the center.

2 Motivating Example

We extend the motivating example of [Andrews \(2018\)](#) from a two-dimensional setting to a high dimensional setting. In this example, Andrews has mirrored clusters over the line $x = -y$, with a single point exactly at $(0, 0)$. This reproduced in a high-dimensional setting, with 150 predictors, 2 groups, 500 observations in each group, and a single centre point. We display the first two components of this data set in Figure 1, which is an example of the relationship between any set of pairwise components in the data.

One would intuitively believe that the probability of the centre point belonging in either cluster would be 50%. However, this is not found to be the case with many clustering algorithms. The k -means algorithm simply labels the point as belonging to one group or another as it is a hard clustering algorithm and hence provides no statistical reference. Conversely, the benchmark expectation-maximization (EM) algorithm, heavily overfits and finds the probability of the centre point belonging to one group to be over 99.999%, and practically 0% to belong the other. This is also an issue within common spectral clustering algorithms, such as those presented in [Löffler et al. \(2021\)](#). Using Algorithm 1 from [Löffler et al. \(2021\)](#) augmented with the EM for a spectral clustering algorithm, we find that it estimates the centre point’s group membership probabilities to be one 100% for one group and 0% for the other. [Andrews \(2018\)](#) has shown that applying a non-parametric bootstrap can address this issue of overfitting in the EM algorithm. However,

in high dimensions, this is extremely slow without some form of dimensionality reduction. [Shreeves and Andrews \(2019\)](#) further expand upon this work by using the non-parametric bootstrap to augment the alternating expectation-conditional maximization (AECM) algorithm. This uses the assumption that the observations arise from a factor analysis model and was developed in a mixture model framework by [Ghahramani et al. \(1996\)](#); [McLachlan and Peel \(2000\)](#) and is further outlined in Section 3.4. While this removes the need for multiple $p \times p$ inversions at each bootstrap iteration, it is still required once per iteration to find the likelihood of the averaged parameter space. Additionally a large number of matrix multiplications are needed to solve for the latent space, slowing the algorithm further.

3 Background

3.1 Finite Mixture Models

FMMs ([McLachlan et al. \(2019\)](#)) are commonly used in the clustering community ([McNicholas \(2016\)](#)) and have been used in a variety of applications; see ([Torres-Carrasquillo et al., 2002](#); [Yu, 2012](#); [Georgiades et al., 2022](#)) for a multitude of uses. A clear benefit of using a FMM for clustering over more common industry techniques, such as the k -means methods and hierarchical trees, is that a FMM provides a statistical representation of the group structure. It also allows for one to compute a probability that an observation belongs in a certain group; a property not available to hard clustering algorithms. They are a convex combination of probability distributions of multiple statistical densities and are expressed as

$$f(\mathbf{x}_i) = \sum_{g=1}^G \pi_g f_g(\mathbf{x}_i \mid \Theta_g). \quad (1)$$

Here \mathbf{x}_i is a p dimensional observation, G is the number of groups/distributions in the model, π_g is the mixing proportion of group g under the constraint $\sum_{g=1}^G \pi_g = 1$, and f_g is the underlying distribution of the g^{th} group component with parameters θ_g . In this work, we focus on mixtures of multivariate normal distributions; that is

$$f(\mathbf{x}_i) = \sum_{g=1}^G \pi_g \phi(\mathbf{x}_i \mid \mu_g, \Sigma_g), \quad (2)$$

where μ_g is the group mean, with covariance Σ_g . However, mixture models have been developed for entire families of other distributions ([Andrews et al., 2011](#); [Franczak et al., 2013](#); [Punzo and McNicholas, 2016](#)). The key benefit of using mixture models over other clustering algorithms is that it is a soft clustering technique, providing a probabilistic interpretation of group membership

for each observation. Let $\mathbf{z}_i = (z_{i1}, z_{i2}, \dots, z_{iG})$ be the G -length vector of probabilities, where $z_{ig} = 1$ if observation i belongs to group g and $z_{ig} = 0$ otherwise. Then π_g can be viewed as the *a priori* probability of observation i belonging to group g , with an *a posteriori* probability of

$$\Pr[z_{ig} = 1 \mid \mathbf{x}_i] = \frac{\pi_g \phi(\mathbf{x}_i \mid \mu_g, \Sigma_g)}{\sum_{j=1}^G \pi_j \phi(\mathbf{x}_i \mid \mu_j, \Sigma_j)}. \quad (3)$$

This can be estimated as

$$\hat{z}_{ig} = \frac{\hat{\pi}_g \phi(\mathbf{x}_i \mid \hat{\mu}_g, \hat{\Sigma}_g)}{\sum_{j=1}^G \hat{\pi}_j \phi(\mathbf{x}_i \mid \hat{\mu}_j, \hat{\Sigma}_j)}, \quad (4)$$

where $\hat{\mu}_g$, $\hat{\Sigma}_g$, and $\hat{\pi}_g$ for all $g = 1, \dots, G$ are the maximum likelihood estimates of the model likelihood

$$\mathcal{L}(\Theta) = \prod_{i=1}^n \sum_{g=1}^G \pi_g \phi(\mathbf{x}_i \mid \mu_g, \Sigma_g). \quad (5)$$

We denote $\ell = \log(\mathcal{L}(\Theta))$ to be the log-likelihood of the model. The finite mixture model requires

$$\underbrace{G-1}_{\text{mixing proportions}} + \underbrace{Gp}_{\text{group means}} + \underbrace{\frac{Gp(p+1)}{2}}_{\text{group covariances}} \quad (6)$$

free parameters, with the parameter contributions displayed below equation 6. The largest contributor arises from the estimation of the group covariance matrices, which is a natural target for parsimony [McNicholas \(2016\)](#). A method to do so is discussed in Section 3.4. However, multiple other techniques have been used to address this; see [Banfield and Raftery \(1993\)](#); [Celeux and Govaert \(1995\)](#); [Tipping and Bishop \(1999\)](#). The most common way to estimate these parameters is in an iterative style, alternating between updating the maximum likelihood estimates and updating the posterior probabilities [Dempster et al. \(1977\)](#). This is known as the expectation-maximization (EM) algorithm and is further detailed in the following section.

3.2 EM Algorithm

The EM algorithm ([Dempster et al., 1977](#); [McLachlan and Krishnan, 2007](#)) is one of the most commonly used methods to estimate FMMs. It iterates between two steps; the expectation (E) step and the maximization (M) step. The E-step calculates the estimated expected value of Z_{ig} for all $i = 1, \dots, n$ and $g = 1, \dots, G$, found in (4), while the M-step calculates the maximum likelihood estimates of $\hat{\pi}_g$, $\hat{\mu}_g$, and $\hat{\Sigma}_g$. Updates for the maximum likelihood estimates given as

$$\hat{\pi}_g = \frac{n_g}{n}, \quad \hat{\mu}_g = \frac{1}{n_g} \sum_{i=1}^n \hat{z}_{ig} \mathbf{x}_i, \quad \& \quad \hat{\Sigma}_g = \frac{1}{n_g} \sum_{i=1}^n \hat{z}_{ig} (\mathbf{x}_i - \hat{\mu}_g)(\mathbf{x}_i - \hat{\mu}_g)'. \quad (7)$$

An algorithm summary from [McNicholas \(2016\)](#) can be written as follows:

1. Initialize \hat{z}_{ig} . Common starts include random group allocation or k-means clustering.
2. While not converged:
 - (a) Update $\hat{\pi}_g = \frac{n_g}{n}$.
 - (b) Update $\hat{\mu}_g = \sum_{i=1}^n \hat{z}_{ig} \mathbf{x}_i$.
 - (c) Update $\hat{\Sigma}_g = \sum_{i=1}^n \hat{z}_{ig} (\mathbf{x}_i - \hat{\mu}_g)(\mathbf{x}_i - \hat{\mu}_g)'$.
 - (d) Update \hat{z}_{ig} .
 - (e) Check convergence criteria. If it is not met, return to 2(a). Otherwise, exit the while loop.

Most convergence criteria used are a form of ‘lack of progress’ criterion, which measure the updated version of the log-likelihood against its previous iteration; that is,

$$|\ell^{(k)} - \ell^{(k-1)}| < \epsilon, \quad (8)$$

for some small, pre-determined value of ϵ . We recommend a pre-set value of $\epsilon = 0.01$; however, this is at the users’ discretion.

3.3 Bootstrapping and the BootEM Algorithm

The bootstrap procedure, introduced in [Efron \(1981\)](#) and [Efron \(1982\)](#), is a resampling technique that allows for providing estimates of standard errors of estimates that otherwise may not be possible to calculate. Specifically, for a parameter θ with estimate $\hat{\theta}$, we can calculate new estimates of $\hat{\theta}$ by sampling with replacement from the data X (referred to as a bootstrap sample). Repeating this process M times, we can compute the standard deviation of the parameter estimate as $\hat{\sigma}_{\hat{\theta}} = \sqrt{\frac{\sum_{j=1}^M (\hat{\theta}_j - \hat{\theta}^*)^2}{M-1}}$ where $\hat{\theta}_j$ corresponds to the estimate from the j^{th} bootstrap sample and $\hat{\theta}^* = \frac{\sum_{j=1}^M \hat{\theta}_j}{M}$ is the averaged parameter estimate. Further, the non-parametric bootstrap sampling technique allows for built-in cross validation, as the non-sampled data from the j^{th} bootstrap sample can be used as a testing set for the j^{th} model.

[Andrews \(2018\)](#) notes that the conventional EM algorithm falls victim to a number of issues. The first of which is that it has the ability to converge to a local maximum, as opposed to the global maximum, in the log-likelihood. This is what one may call an underfitting of the model, as the likelihood-optimal estimates are not achieved. The other common issue is that it will overfit to the data available at times, resulting in the optimal log-likelihood but having overconfident group membership estimates, as was shown in our motivating example.

This can be addressed by evaluating EM algorithms over repeated bootstrap samples of the original data matrix and estimating the out-of-bag (OOB) group memberships for observations left

out of the sample. Additionally, the parameter estimates are averaged over the multiple bootstrap iterations, preventing the convergence to a local maximum. It should be noted that these averaged parameter estimates are not maximum likelihood estimates; although the final likelihoods are very similar. As a result, conventional lack of progress criterion cannot be used to determine the stopping point in the algorithm. Instead, it is assumed that once the algorithm has converged once the last M log-likelihood values return a null from result from the Durbin-Watson test; a test for auto-correlation over a set of indices. When this is achieved, it is assumed that the algorithm has converged and deviations in the likelihood are due to the randomness from the bootstrap sampling.

An algorithm summary regarding the BootEM algorithm is as follows:

1. Construct an initial cluster membership $\mathbf{z}^{(0)}$, set $k = 1$ to be the bootstrap index
2. While not converged:
 - (a) Take a non-parametric bootstrap $X^{(k)}$ and take corresponding cluster memberships from $\mathbf{z}^{(k-1)}$
 - (b) Perform EM algorithm on $X^{(k)}$ using $\mathbf{z}^{(k-1)}$ as cluster initialization
 - (c) Check convergence criteria. If it is not met return to 2(a), otherwise exit the loop

While this algorithm may appear to be intuitive and simple in construction, [Andrews \(2018\)](#) has shown it to properly address the issues of converging to solutions corresponding to local maxima through a series of simulations and real data analyses. However due to the bootstrapping procedure and the use of the Durbin-Watson test as a convergence criteria, it is also possible that this algorithm may take an unreasonably large amount of iterations to converge, or not converge at all. These issues are addressed in Section 3.3 of [Andrews \(2018\)](#).

3.4 BootAECM Algorithm

The factor analysis model assumes that the p -dimensional observation \mathbf{x}_i arises from

$$\mathbf{x}_i = \mu + \Lambda \mathbf{u}_i + \epsilon_i, \quad (9)$$

where μ is a p -dimensional mean vector, Λ is a $p \times q$ matrix of factor loadings, $\mathbf{u}_i \sim N(0, \mathbf{I}_q)$ is a q -dimensional vector of latent variables, and $\epsilon_i \sim N(0, \Psi)$ where Ψ is a $p \times p$ diagonal matrix. As a result, it can be shown that the marginal distribution for \mathbf{x}_i is $\phi(\mathbf{x}_i \mid \mu, \Lambda\Lambda' + \Psi)$. This methodology was applied to the field of mixture models ([Ghahramani et al., 1996](#); [McLachlan and Peel, 2000](#)) and named “mixtures of factor analyzers.” The reason for using this method over the conventional finite mixture model is two-fold; (1) it allows one to find underlying factors of groups and (2) the computational benefits in terms of both storage and run time are needed for moderate-to-high

dimensional data sets. This is due to the fact that the number of free parameters to be estimated is reduced and the evaluation of $\hat{\Sigma}^{-1}$ and $|\hat{\Sigma}|$ are avoided. Under a fully unconstrained mixture of factor analyzers model, the number of free parameters is reduced to

$$G[pq - q(q - 1)/2] + Gp. \quad (10)$$

The key difference between (6) and (10) is that the p^2 term - the main source of free parameters - no longer exists in (10). Additionally, this implementation does not require multiple inversions of the $p \times p$ covariance matrix for the calculation of the likelihood. These calculations are instead approximated using the latent subspace, reducing computation time. For more information regarding the computational aspects of the AECM algorithm, readers may refer to McNicholas (2016).

This algorithm was implemented in a bootstrap framework, similar to that of Section 3.3, by Shreeves and Andrews (2019). This allows for the use of the algorithm in moderate-to-high dimensional settings; something that was not initially possible with BootEM due to the reasons stated above.

3.5 Spectral Clustering

Spectral clustering is, in a broad sense, the act of performing a clustering algorithm after a data set has undergone spectral decomposition resulting in a dimensionality reduction. It is not unfounded to perform a spectral decomposition on the data matrix itself, see Kannan et al. (2009) and Kumar and Kannan (2010). One type of spectral decomposition commonly used, and the one we use in this paper, is a singular value decomposition (SVD). Mathematically, SVD is an operation decomposes an $m \times n$ matrix X into the matrix multiplication $X = USV^\top$. Here, U is an $m \times m$ unitary matrix, V is a $n \times n$ (complex) unitary matrix, and S (typically written as Σ , however we write as S to avoid confusion with respect to our previously discussed covariance matrix) is a non-negative diagonal matrix containing the singular values of X along the diagonal. The amount of non-zero singular values is equal to the rank of X . Often, SVD is performed such that the singular values of X along the diagonal of S are in decreasing order, and we maintain this convention here.

In this paper, we follow the method of Algorithm 1 from Löffler et al. (2021). There, the authors' perform SVD on a $p \times n$ data matrix X (outside of this section, we assume the data matrix to be $n \times p$) and then perform a k -means clustering on the matrix product $\hat{Y} = U_G^\top X$, where U_G is composed of the first G columns of the unitary matrix from the SVD for X . This technique reduces the original $n \times p$ data matrix to one that is $n \times G$. In a high dimensional framework, where SVD would be performed, this significantly reduces the dimensionality of the data. By clustering on \hat{Y} , the spectral gap condition (Von Luxburg (2007), Löffler et al. (2021)) can be removed. We adjust

Algorithm 1 from [Löffler et al. \(2021\)](#) by using an EM algorithm to construct a Gaussian mixture model instead of using k -means to perform the clustering after the dimensionality reduction. We call this the Spectral-EM algorithm. This allows for a more granular statistical interpretation of the resulting fitted model. Using spectral algorithms to construct mixture models is not unfounded; specifically, [Vempala and Wang \(2004\)](#) show that simple spectral clustering algorithms are able to achieve success in learning Gaussian mixture models under minor assumptions.

4 Methodology

4.1 Bootstrapped Spectral Clustering

We present two algorithms to address overfitting in a spectral clustering algorithm. By utilizing the spectral decomposition procedure from [Löffler et al. \(2021\)](#) and the bootstrapping procedure employed by [Andrews \(2018\)](#), our algorithms incorporate dimensionality reduction and the bootstrapping procedure. This allows for not only increased computational speed, but also a reduction in overfitting to the data. These algorithms are presented in Sections [4.1.1](#) and [4.1.2](#).

4.1.1 Spectral-BootEM

The first algorithm is an adjustment of the algorithm original developed by [Andrews \(2018\)](#). In our adjustment, we perform an SVD on the transpose of the $n \times p$ data matrix X and then perform the non-parametric bootstrap on $\hat{Y} = XU_G$ in addition to altering the convergence criteria. The algorithm takes the following form.

1. Perform SVD on X^\top , and compute $\hat{Y} = XU_G$
2. Construct an initial cluster membership for \hat{Y} , denoted as $\mathbf{z}^{(0)}$ and set the bootstrap index $k = 1$
3. While not converged:
 - (a) Take a bootstrap sample of \hat{Y} , denote as $\hat{Y}^{(k)}$ and take the corresponding cluster memberships from $\mathbf{z}^{(k-1)}$
 - (b) Perform EM algorithm on $\hat{Y}^{(k)}$ with $\mathbf{z}^{(k-1)}$ as initialization to compute parameter estimates
 - (c) Compute the average parameter space and check convergence criteria. If it is not met, return to 3(a). Otherwise, exit the loop

This algorithm will be referred to as the Spectral Bootstrapped EM, or Spectral-BootEM for short, for the remainder of this paper. We modify the convergence criteria from the method proposed

by Andrews (2018), where the Durbin-Watson test is used to check for auto-correlation. In the modification, convergence is determined by computing the component-wise relative difference in the averaged parameter between iterations space divided by the number of free parameters. Specifically, if we denote the k^{th} relative difference in averaged parameter space by $R_\theta^{(k)}$, convergence is achieved when

$$\frac{R_\theta^{(k)}}{G - 1 + Gp + Gp(p + 1)/2} < \epsilon_B, \quad (11)$$

where ϵ_B is a small, user-defined value and not necessarily equal to the ϵ used for convergence discussed in Section 3.2. Written algebraically, this takes the form

$$R_\theta^{(k)} = \sum_{g=1}^G \left| \frac{\hat{\pi}_g^{*,(k)} - \hat{\pi}_g^{*,(k-1)}}{\hat{\pi}_g^{*,(k-1)}} \right| + \sum_{g=1}^G \sum_{j=1}^p \left| \frac{\hat{\mu}_{j,g}^{*,(k)} - \hat{\mu}_{j,g}^{*,(k-1)}}{\hat{\mu}_{j,g}^{*,(k-1)}} \right| + \sum_{g=1}^G \sum_{j=1}^p \sum_{k=j}^p \left| \frac{\hat{\sigma}_{j,k,g}^{*,(k)} - \hat{\sigma}_{j,k,g}^{*,(k-1)}}{\hat{\sigma}_{j,k,g}^{*,(k-1)}} \right|. \quad (12)$$

Here, $\hat{\pi}^{*,(k)}$, $\hat{\mu}^{*,(k)}$ and $\hat{\sigma}^{*,(k-1)}$ represent the averaged mixing proportion, mean, and covariance, respectively, from the k^{th} bootstrap sample. For the diagonal components of the covariance matrix (i.e. when $j = k$), this is interpreted the estimate variance. When computing the component wise relative differences in the covariance matrices, we do not include the lower triangles of the group matrices, as these are symmetric and hence the off-diagonal components would be contributing twice to the relative difference. In both (11) and (12), we have written p to represent the dimensions. However, in the case of spectral clustering, p is reduced down to G ; hence these equations would be adjusted accordingly, substituting a G for any p .

4.1.2 Boot-Spectral

The second algorithm we propose is a substantially different adjustment from that of Andrews (2018). After creating the bootstrap sample, \hat{X} , SVD is then performed on the sampled matrix and $\hat{Y} = \hat{X}U_G$ is computed. The rest of the bootstrap EM is then continued algorithm as in Andrews (2018). With this method, a new SVD is computed for each sample. However, as SVD is not a unique operation, we order our singular values in S in descending order, and are sampling from the same data matrix X . The SVD is expected to be similar enough to allow for a reputable model, while creating enough diversity in model fitting to address the issue of overfitting. The algorithm is as follows:

1. Perform SVD on X^\top and compute $\hat{Y} = XU_G$
2. Construct an initial cluster membership for \hat{Y} , denoted as $\mathbf{z}^{(0)}$ and set the bootstrap index $k = 1$
3. While not converged:
 - (a) Take a non-parametric bootstrap sample from X , denote $\tilde{X}^{(k)}$

- (b) Perform SVD on $\left(\tilde{X}^{(k)}\right)^\top$ to compute $\tilde{Y}^{(k)} = \tilde{X}^{(k)}U_G$ and take corresponding cluster memberships from $\mathbf{z}^{(k-1)}$
- (c) Perform EM algorithm on $\tilde{Y}^{(k)}$ with $\mathbf{z}^{(k-1)}$ as initialization to compute group parameter estimates
- (d) Compute group memberships and log-likelihood from parameter estimates for \hat{Y}
- (e) Compute the average parameter space and check convergence criteria. If it is not met, return to 3(a). Otherwise, exit the while loop.

As in the Spectral-BootEM algorithm, lack of progress in the parameter space is again used as the convergence criteria. We call this algorithm the Bootstrapped Spectral Clustering algorithm, or BootSpectral for short. Additionally, we set a minimum amount of bootstrap samples for both algorithms as a burn-in period for the averaged parameter space. While it is up to the user to specify the length of the burn-in, we suggest a minimum of 300 bootstrap samples, however for many problems more bootstrap samples are likely needed. We compare this algorithm to Spectral BootEM, as well as the standard spectral clustering, BootEM, EM, and BootAECM algorithms in Section 4.

With both of the above algorithms we can compute out-of-bag group membership estimates, which provide a more statistically favourable interpretation of the results. It assumes that an observation omitted from the bootstrap sample has not been observed, resulting in a built-in cross validation technique. As discussed by Andrews (2018), it is possible that the out-of-bag estimates do not match the final averaged estimated model group estimates. Further, as both algorithms perform clustering on variants of \hat{Y} , we are not concerned with the spectral gap.

4.2 Potential Issues

With all dimensionality reduction techniques, there is a risk in losing a non-trivial amount of the variance within the original data. Our spectral decompositions are no exception. In data with geometrically close groups, a loss of variance due to a dimensionality reduction poses a potential to not fit one or more groups. Further, taking a bootstrap sample leaves out, on average, one third of the original data. While this allows for a natural cross-validation of the fitted model, it also poses the issue in the event that there exists a small sized group, comparative to n . As such, when taking a bootstrap sample there is a risk that not enough observations from potential groups are sampled, resulting either in empty groups or unrealistic parameter estimates. These are well known problems in the clustering community, of which many algorithms are prone to including our algorithms presented in Sections 4.1.1 and 4.1.2.

5 Results

5.1 Simulations

5.1.1 Mirror Data

We begin by going back to our mirror data set, first presented in Section 2. While it is difficult to compare log-likelihood values between our proposed algorithms and the non-spectral algorithms due to the dimensionality reduction, the key metrics of interest are run times, number of bootstrap samples required, and the estimated probability vectors for the centre point. The two novel algorithms are applied and compared to the EM, SpectralEM, BootEM, and BootAECM in Table 1. We also view the probability vector for group membership of the centre point, and denote this as \mathbf{z}_c as well as the out-of-bag group membership for the centre point, in the column ‘OOB \mathbf{z}_c ’. A seed is set for reproducibility. Additional settings include $\epsilon = 0.1$ for all EM convergence parameters, $\epsilon_B = 0.001$ for the Spectral-BootEM and BootSpectral convergence parameters, and the Durbin-Watson p-value is equal to 0.05 for the BootEM algorithm.

	\mathbf{z}_c	OOB \mathbf{z}_c	log-likelihood	Bootstraps	Elapsed Time (s)
EM	[0, 1]	-	-202011.6	-	0.301
AECM	[0, 1]	-	-214085.7	-	1.81
SpectralEM	[0, 1]	-	-4657.0	-	0.074
BootEM	[0.490, 0.510]	[0.506, 0.494]	-202441.8	4202	3769.097
BootAECM	[0.422, 0.578]	[0.475, 0.525]	-214244.2	500	415.56
Spectral-BootEM	[0.498, 0.502]	[0.493, 0.507]	-5022.308	1186	128.447
BootSpectral	[0.503, 0.497]	[0.496, 0.504]	-5021.03	2659	450.017

Table 1: Comparative results for high-dimensional mirror data.

Analyzing Table 1, we see that the EM, AECM, and SpectralEM algorithms heavily overfit to the data, as they are classifying the centre point as belonging exclusively to a single group. Both these algorithms are incredibly fast though, and require few bootstrap samples for convergence when compared to the bootstrapped counterparts, with the SpectralEM algorithm being non-trivially quicker due to its dimensionality reduction. Looking next at the BootEM algorithm, we see that this takes the most bootstrap samples and longest time to complete, performing at a speed of 1.1 bootstrap samples per second. It does succeed in addressing the overfitting issue as both the model and OOB group membership probabilities produce the more intuitive answer for the centre point. Unlike the EM algorithm, BootEM does not converge to the global maximum as is shown by its lower log-likelihood, a result more thoroughly discussed by Andrews (2018). The BootAECM again addresses the overfitting issue and requires significantly fewer bootstrap samples to complete than the BootEM case, however the returned probability vector is the furthest from the intuitive [0.5, 0.5] for the bootstrapped algorithms. It performs at a speed of 1.2 bootstrap samples per second, a slight improvement over the BootEM algorithm. Analyzing

our first novel algorithm, the Spectral-BootEM, we see that this addresses the convergence to local maxima and overfitting issue of the original SpectralEM, as shown by the Spectral-BootEM’s group membership probabilities and log-likelihood values. It required 1186 bootstrap samples and completed in 128.447 seconds, attaining a speed 9.2 bootstrap samples per second. This is an impressive increase in computational speed over both the BootEM and BootAECM and is due to the significant dimensionality reduction that is performed. Our next novel algorithm, the BootSpectral algorithm, also addresses overfitting, achieving a similar log-likelihood as the Spectral-BootEM and arguably equivalent group membership probabilities for both the actual memberships and OOB memberships for the centre point. It performed in 2659 bootstrap samples and completed approximately 6.0 bootstrap samples per second, a decreases in speed from the Spectral-BootEM. This is due to the fact that BootSpectral is computing a unique SVD for each bootstrap sample, resulting in a more computationally expensive process. In contrast, Spectral-BootEM computes an SVD only once, and this is also the reason for the greater amount of iterations required to reach convergence. This motivating example demonstrates that the novel algorithms address the issues of overfitting and converging to a local maxima in a high-dimensional setting. In addition, it achieves a significant decrease in time required to find a solution; a benefit that compounds in higher dimensions.

To further investigate the convergence and speed of our algorithm, we run the BootEM, Spectral-BootEM, and BootSpectral algorithms on the mirror data 5 times with varying seeds. All other input parameters are the same as before. The speed at which these algorithms reach convergence and the required number of bootstrap samples to do this are displayed in Table 2a.

Algorithm	Run 1	Run 2	Run 3	Run 4	Run 5
BootEM	1575.210	482.769	448.512	722.639	2540.199
Spectral-BootEM	99.306	127.603	78.259	60.740	97.106
BootSpectral	401.097	520.417	181.603	221.718	318.404

(a) Time (s) to reach convergence using a two-group solution in mirror data. Each algorithm was ran 5 times to evaluate convergence consistency.

Algorithm	Run 1	Run 2	Run 3	Run 4	Run 5
BootEM	1733	562	500	842	2836
Spectral-BootEM	856	1174	714	554	923
BootSpectral	2350	2956	1182	1428	1970

(b) Bootstrap samples required for convergence using a two group solution in mirror data. Each algorithm was ran 5 times to evaluate convergence consistency.

Table 2

It can be seen that that the BootEM consistently takes the longest time to reach convergence, and even its quickest run is longer than the slowest run of Spectral-BootEM and four of the five runs of BootSpectral. We find that Spectral-BootEM is consistently the fastest algorithm to reach convergence its defined convergence criteria, with BootSpectral being slower than Spectral-

BootEM but still much quicker than the standard BootEM. Table 2b shows that the required samples for the BootEM to reach convergence is fairly sporadic in nature, as in run 3 it reaches convergence at its minimum amount of 500 samples while run 5 takes over 2800 samples. Again, Spectral-BootEM is the most consistent of the three algorithms. Interestingly, BootSpectral in run 2 requires the most samples out of all runs for each algorithm to reach convergence. This is due to the fact that BootSpectral recomputes its SVD for each bootstrap sample which compounds the variation (or lack there of) in the sample, and hence certain sample estimates may act as outliers impacting the averaged parameter space more significantly than others. We conclude that that our novel bootstrapped spectral clustering algorithms and convergence criteria generally produce more consistent results when compared to the BootEM.

5.1.2 Cross-Over Data

The next case study is on a simulated data set, which will be referred to as call the cross-over data set. We create a two group longitudinal data set where at the halfway point, the groups cross over one another, as demonstrated in Figure 2. We have one group trending down, and another trending upwards. In our case, we have 150 observations in each group with values observed at whole number increments from one to 41. The first group mean travels from -20 to 20 by an increment of one per time step, while the second group mean travels from 20 to -20 again by an increment of one per time step. The covariance matrix for each group is constructed to be 1 on the diagonal and 0.9 on the off-diagonal. Observations are simulated using a multivariate normal distribution. Three observations are then created which belong to the bottom group for the first 20 time points, and join the other group at the cross-over event, continuing on the new path (see Figure 3). We refer to this as the cross-over data set. The EM and SpectralEM algorithm both overfit to this data, and as was seen in the mirror simulation from Section 5.1.1, assign a group probability vector to each group changing observation of $[1, 0]$, a clear overfit as it is clear that an intuitive and *true* solution would be closer to a group probability vector of $[0.5, 0.5]$, as was the case with the mirror data.

We run three experiments to demonstrate the versatility of our convergence criteria, and compare it to the results of the BootEM algorithm. For both the Spectral-BootEM and BootSpectral, the model is fitted using the cross-over data set with ϵ_B set to 0.01, 0.005, and 0.0001. The resulting group probability vectors for the group changing observations are analyzed in Tables 3, 4, and 5. For all cases, we set the the burn-in to be 300 bootstrap samples. The group changing observations are denoted as *Obs 1*, *Obs 2*, and *Obs 3*. We further analyze the convergence of the averaged parameter space of Spectral-BootEM and BootSpectral in Figures 4 and 5, respectively.

Analyzing first Table 3, where $\epsilon_B = 0.01$, we see that the Spectral-BootEM still partially over-

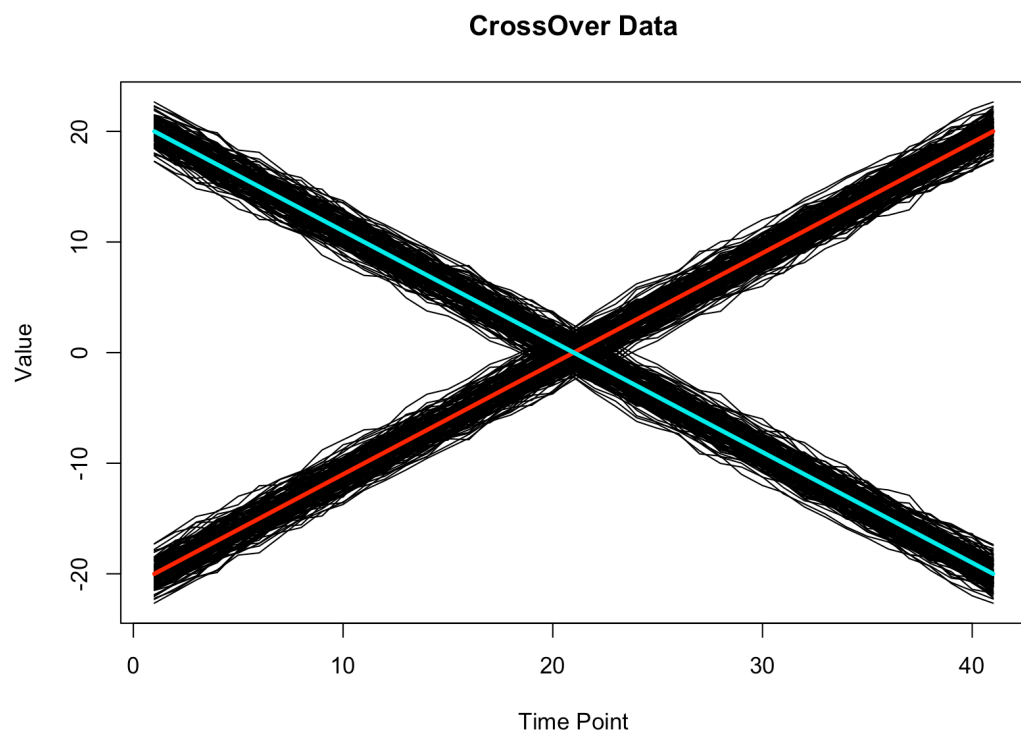


Figure 2: Cross-over data with group means indicated in red and blue.

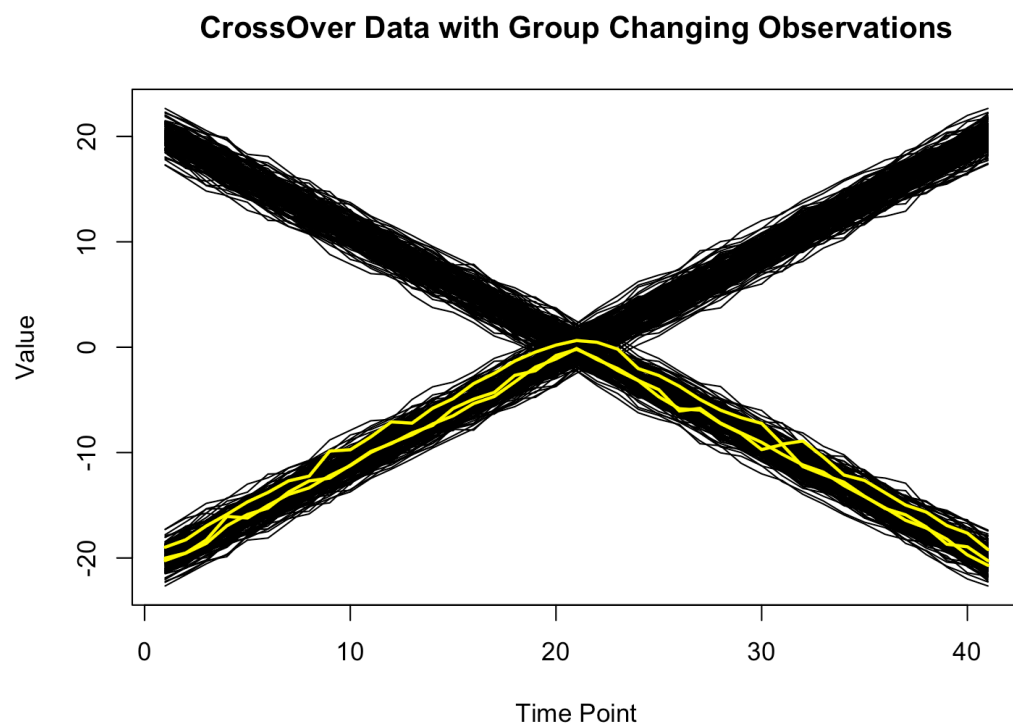


Figure 3: Cross-over data with group changing observations indicated in yellow.

	Spectral-BootEM \mathbf{z}_i	BootSpectral \mathbf{z}_i	BootEM \mathbf{z}_i
Obs 1	[0.703, 0.297]	[0.620, 0.380]	[0.493, 0.507]
Obs 2	[0.710, 0.290]	[0.617, 0.383]	[0.446, 0.554]
Obs 3	[0.707, 0.293]	[0.620, 0.380]	[0.490, 0.510]

Table 3: Averaged \mathbf{z} vectors for group changing observations with $\epsilon_B = 0.01$.

	Spectral-BootEM \mathbf{z}_i	BootSpectral \mathbf{z}_i	BootEM \mathbf{z}_i
Obs 1	[0.490, 0.510]	[0.577, 0.423]	[0.493, 0.507]
Obs 2	[0.480, 0.520]	[0.573, 0.427]	[0.490, 0.510]
Obs 3	[0.487, 0.513]	[0.573, 0.427]	[0.490, 0.510]

Table 4: Averaged \mathbf{z} vectors for group changing observations with $\epsilon_B = 0.005$.

	Spectral-BootEM \mathbf{z}_i	BootSpectral \mathbf{z}_i	BootEM \mathbf{z}_i
Obs 1	[0.487, 0.513]	[0.509, 0.491]	[0.493, 0.507]
Obs 2	[0.485, 0.515]	[0.506, 0.494]	[0.490, 0.510]
Obs 3	[0.486, 0.514]	[0.508, 0.492]	[0.490, 0.510]

Table 5: Averaged \mathbf{z} vectors for group changing observations with $\epsilon_B = 0.0001$.

fits to the data, as is shown by the poor probabilities in the group probability vectors. Meanwhile, the BootSpectral algorithm performs well, with group probability vectors close to $[0.5, 0.5]$. The BootEM also performs admirably, and much better than Spectral-BootEM. However, as our convergence criteria allows for flexibility in ϵ_B , we lower this to 0.0005, and display these results in table 4. Immediately we see a significant reduction of overfitting in the Spectral-BootEM algorithm, and a slight decrease in performance of BootSpectral. We further note that BootEM remains unchanged, as it's convergence criteria uses a Durbin-Watson test for auto-correlation, and as such does not allow for any flexibility. It is also notable that the adjustment of the significance level for the Durbin-Watson test rarely has any affect on when the algorithm converges, since the final p-value is often far below the threshold of $\alpha = 0.05$.

Next, the convergence criteria is again reduced such that the relative difference (scaled by the number of free parameters) in the average parameter space cannot exceed 0.0001, and display the results in Table 5. Here, we find the most intuitively logical results for Spectral-BootEM and BootSpectral, as both provide group probability vectors close to $[0.5, 0.5]$ for all changing observations. This demonstrates the flexibility of the convergence criteria.

We now analyze the behaviour of convergence criteria in the algorithm runs, shown for Spectral-BootEM in Figure 4 and BootSpectral in Figure 5. First analyzing Spectral-BootEM in Figure 4, we see that setting $\epsilon_B = 0.0001$ results in the most iterations, as is to be expected, and achieves an asymptotic behaviour demonstrating that any extreme bootstrapped samples will have a small impact on the overall averaged parameter space; something which has been found to significantly impact the convergence BootEM algorithm. The results are analogous for the BootSpectral, which we show in Figure 5. We note in both figures, a large ϵ_B results in extremely fast convergence, and

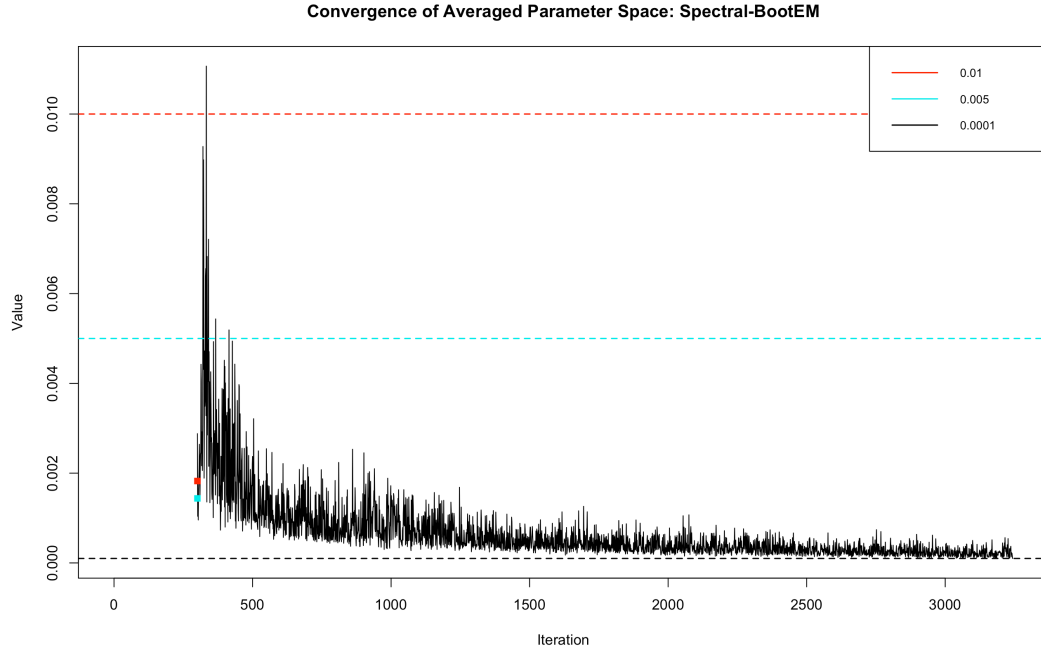


Figure 4: Impact of convergence parameter ϵ_B on convergence rate of averaged parameter space in Spectral-BootEM.

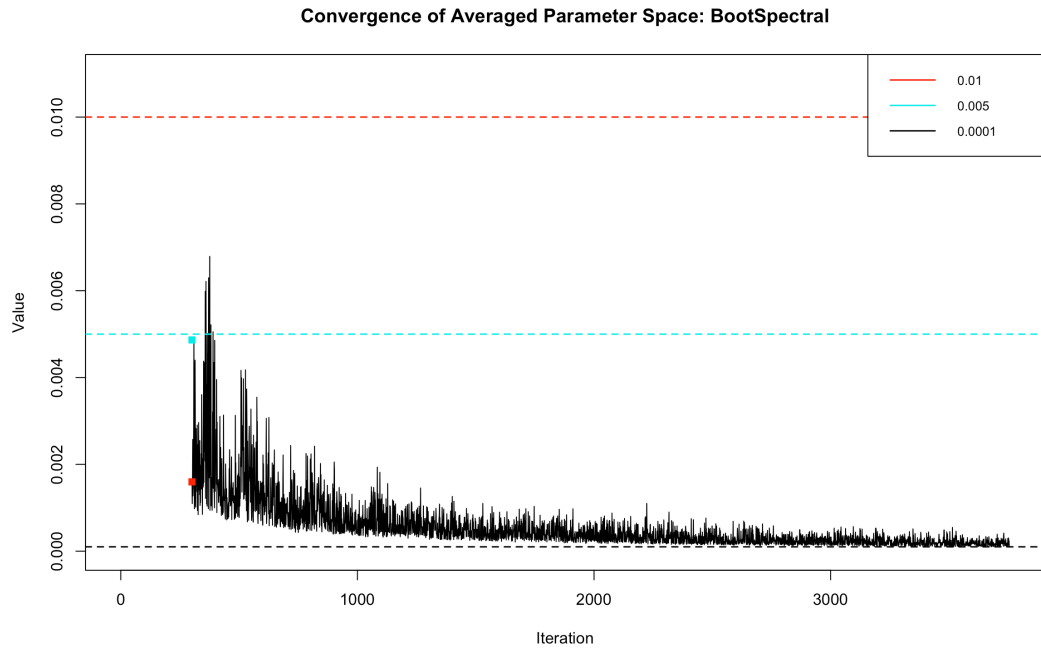


Figure 5: Impact of convergence parameter ϵ_B on convergence rate of averaged parameter space in BootSpectral.

hence we have little data to show. As we do not begin checking for convergence before iteration 300, it is possible that our algorithms could converge earlier for less strict values of ϵ_B , however to avoid potential overfits we maintain that a minimum of 300 bootstraps samples is required for burn-in. We note that in Figure 4, despite the convergence measure being below 0.005 for multiple iterations, extreme bootstrap samples significantly impact the averaged parameter space, and we see a large spike occurring early in the convergence measure growing to larger than 0.01. This is despite it being relatively small to begin with, as our two other runs with larger ϵ_B values had already converged. As such, we find the choice of ϵ_B to be of great importance to achieve a stable averaged parameter space. These figures also show the importance of suitable burn-in period, in order to avoid any significant spikes in the relative difference of the averaged parameter space between iterations in the early stages of the bootstrapped model estimation.

5.2 Real Data

5.2.1 Raman Data

Raman spectroscopy (McCreery, 2005) is an optical interrogation method which consists of using inelastic light scattering to identify constituent chemicals by their vibrational modes. The acquired spectra can therefore provide detailed information on a range of constituents within a single sample acquisition. Changes in the positioning of peaks, as well as their relative amplitudes, can be used to identify the change in molecular dynamics due to a particular perturbation of a system.

Matthews et al. (2015) collected a series of Raman spectra that are classified into three different groups; lung (H460), breast (MCF-7), and prostate (LNCaP) tumor cells. Their research identified that using dimensionality reduction techniques, such as principal component analysis, is a potential way to identify the discrepancies between different cell types while also monitoring the underlying biochemical changes within given cell lines. Specifically, they found that one can distinguish the lung and breast tumor cells from the prostate tumor cells through the levels of glycogen found in their underlying spectra. Deng et al. (2020) further verified this using a variety of dimensionality reduction techniques, such as nonnegative matrix factorization and nonnegative least squares, comparing the results to those previously found by Matthews et al. (2015). Additionally, they were able to identify both glycogen and lipid-like components to further discern the disparity between different cell lines. Herein, we elect to utilize our novel methodology to identify the underlying groups structure under the assumption that there is no group information available.

The data consists of 1080 observations in the 381-dimensional space. Here each observation consists of a series of Raman intensities (arbitrary units) at specific wavenumbers (cm^{-1}). Figure 6 displays the collection of observations in our data set coloured in grey. Additionally, we include the group means which identify the averaged spectra for the H460 (red), MCF-7 (blue), and LNCaP

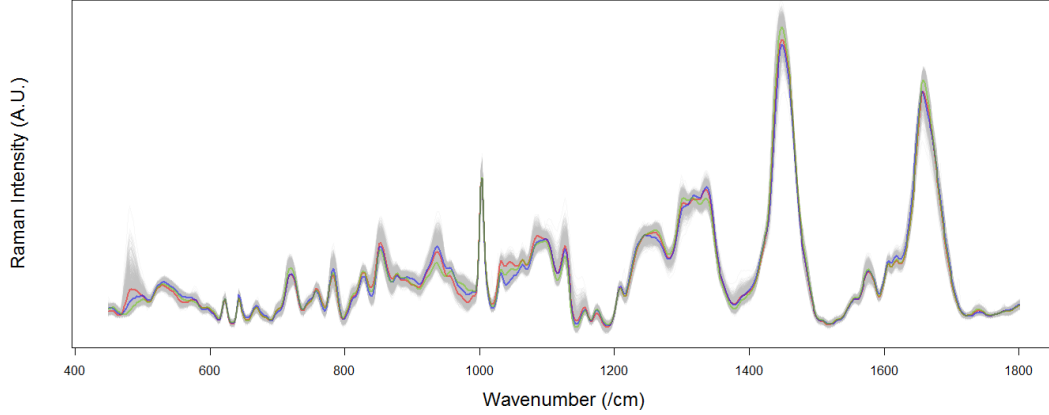


Figure 6: A demonstration of observations in the Raman spectroscopy data set. Observations are coloured in grey, whereas the group means are displayed in red, green, and blue.

(green) cell lines. Each group has an even number (360) of observations, which are differentiated by radiation dose, number of days, and individual number; all of which are left out of the clustering model.

	CR	ARI	log-likelihood	Bootstraps	Elapsed Time
AECM	1.00	1.00	3,648,714	-	2000.84
SpectralEM	0.99	0.98	21,270.54	-	0.83
Spectral-BootEM	0.99	0.98	21,250.56	300	53.75
BootSpectral	0.99	0.97	20,874.64	300	195.55

Table 6: Comparative results for Raman spectroscopy data. Classification rate (CR) and adjusted Rand index (ARI) are both measures of agreement between true classes and the assigned cluster memberships.

Table 6 displays results from the Spectral-EM algorithm and its bootstrapped counterparts on the Raman spectroscopy data set. These results include the percentage of correctly classified observations (CR), the adjusted rand indices (ARI; [Morey and Agresti \(1984\)](#)), log-likelihoods, number of bootstrap iterations, and elapsed run time of the algorithms. While the conventional Spectral-EM performs well, it should be noted that both the Spectral-BootEM and BootSpectral algorithms also achieve similar results. This is indicative of a clear solution in the data. However, it should be noted that this clustering problem is not feasible using the conventional EM algorithm, its bootstrapped counterpart, or the BootAECM due to the requirement of $p \times p$ matrix inversions; an operation that often results in computational errors. This is due to the fact that matrix singularities arise from a deficient number of observations within groups and is further compounded when taking into consideration the data left out in a bootstrapped sample. While the conventional AECM algorithm does not require a $p \times p$ matrix inversions, its bootstrapped version does since it requires an inversion of the averaged sample space covariance matrix. This cannot be avoided as an inversion using the averaged latent parameters can be perturbed due to discoveries of different

orthogonal rotations in the data. The conventional AECM algorithm performs admirably, with a perfect classification rate and ARI. However, its elapsed run time is over ten times the next slowest algorithm in table 6. While it is the user’s decision to decide which algorithm is more appropriate, the expense of a few misclassifications in exchange for much faster run time was deemed worthy in this case. Further, the using the bootstrapped algorithms assuage concern of overfitting to the data, something that is a more likely in AECM algorithm given its perfect classification rate.

6 Conclusion

We have demonstrated that our two novel bootstrapped spectral clustering algorithms effectively and efficiently address the issue of overfitting. These algorithms have shown to achieve a significant boost in speed without a loss in accuracy from the dimensionality reduction. Comparing the novel methods to two previously bootstrap augmented clustering algorithms demonstrated advantageous results in both simulation studies and real data applications. Our choice of convergence measure by way of the relative difference in the averaged parameter space allows for a more consistent model solution than other convergence criteria methods, such as the Durbin-Watson test.

We do not explicitly state which algorithm is preferred, as it is dependent on the clustering problem and underlying data. The Spectral-BootEM is easier to interpret and less likely to result in substantial deviations in the averaged parameter space for each bootstrapped model, while the BootSpectral allows for the discovery of latent spaces that may not be immediately obvious in the full data set. This results in greater variation of the fitted models of each bootstrap, causing full exploration of the parameter space. Either of these characteristics may be desirable for certain problems, and is the choice of algorithm is dependent on the original variability within the data and are dependent on the users’ desired tasks.

7 Acknowledgements

The authors kindly thank Dr. Jeffrey Andrews for providing infrastructure allowing for a more streamlined research process. The authors also thank Dr. Jeffrey Andrews and Dr. Ryan Browne for permission to use the cross-over data simulation example. Finally, we thank Dr. Andrew Jirasek and his medical physics research group for permission to use the Raman Spectroscopy data.

References

- Andrews, J. L. (2018). Addressing overfitting and underfitting in gaussian model-based clustering. *Computational Statistics & Data Analysis*, 127:160–171.
- Andrews, J. L., McNicholas, P. D., and Subedi, S. (2011). Model-based classification via mixtures of multivariate t-distributions. *Computational Statistics & Data Analysis*, 55(1):520–529.
- Banfield, J. D. and Raftery, A. E. (1993). Model-based gaussian and non-gaussian clustering. *Biometrics*, pages 803–821.
- Bouveyron, C. and Brunet-Saumard, C. (2014). Model-based clustering of high-dimensional data: A review. *Computational Statistics & Data Analysis*, 71:52–78.
- Celebi, M. E. and Aydin, K. (2016). *Unsupervised learning algorithms*. Springer.
- Celeux, G. and Govaert, G. (1995). Gaussian parsimonious clustering models. *Pattern recognition*, 28(5):781–793.
- Dempster, A. P., Laird, N. M., and Rubin, D. B. (1977). Maximum likelihood from incomplete data via the em algorithm. *Journal of the Royal Statistical Society: Series B (Methodological)*, 39(1):1–22.
- Deng, X., Ali-Adeeb, R., Andrews, J. L., Shreeves, P., Lum, J. J., Brolo, A., and Jirasek, A. (2020). Monitor ionizing radiation-induced cellular responses with raman spectroscopy, non-negative matrix factorization, and non-negative least squares. *Applied spectroscopy*, 74(6):701–711.
- Efron, B. (1981). Nonparametric estimates of standard error: the jackknife, the bootstrap and other methods. *Biometrika*, 68(3):589–599.
- Efron, B. (1982). *The jackknife, the bootstrap and other resampling plans*. SIAM.
- Franczak, B. C., Browne, R. P., and McNicholas, P. D. (2013). Mixtures of shifted asymmetric laplace distributions. *IEEE Transactions on Pattern Analysis and Machine Intelligence*, 36(6):1149–1157.
- Georgiades, S., Tait, P. A., McNicholas, P. D., Duku, E., Zwaigenbaum, L., Smith, I. M., Bennett, T., Elsabbagh, M., Kerns, C. M., Mirenda, P., et al. (2022). Trajectories of symptom severity in children with autism: Variability and turning points through the transition to school. *Journal of autism and developmental disorders*, 52(1):392–401.
- Ghahramani, Z., Hinton, G. E., et al. (1996). The EM algorithm for mixtures of factor analyzers. Technical report, Technical Report CRG-TR-96-1, University of Toronto.

- Kannan, R., Vempala, S., et al. (2009). Spectral algorithms. *Foundations and Trends® in Theoretical Computer Science*, 4(3–4):157–288.
- Kumar, A. and Kannan, R. (2010). Clustering with spectral norm and the k-means algorithm. In *2010 IEEE 51st Annual Symposium on Foundations of Computer Science*, pages 299–308. IEEE.
- Löffler, M., Zhang, A. Y., and Zhou, H. H. (2021). Optimality of spectral clustering in the gaussian mixture model. *The Annals of Statistics*, 49(5):2506–2530.
- Matthews, Q., Isabelle, M., Harder, S. J., Smazynski, J., Beckham, W., Brolo, A. G., Jirasek, A., and Lum, J. J. (2015). Radiation-induced glycogen accumulation detected by single cell raman spectroscopy is associated with radioresistance that can be reversed by metformin. *PloS one*, 10(8):e0135356.
- McCreery, R. L. (2005). *Raman spectroscopy for chemical analysis*. John Wiley & Sons.
- McLachlan, G. and Peel, D. (2000). Mixtures of factor analyzers. In *In Proceedings of the Seventeenth International Conference on Machine Learning*. Citeseer.
- McLachlan, G. J. and Krishnan, T. (2007). *The EM algorithm and extensions*. John Wiley & Sons.
- McLachlan, G. J., Lee, S. X., and Rathnayake, S. I. (2019). Finite mixture models. *Annual review of statistics and its application*, 6:355–378.
- McNicholas, P. D. (2016). *Mixture model-based classification*. Chapman and Hall/CRC.
- Morey, L. C. and Agresti, A. (1984). The measurement of classification agreement: An adjustment to the rand statistic for chance agreement. *Educational and Psychological Measurement*, 44(1):33–37.
- Punzo, A. and McNicholas, P. D. (2016). Parsimonious mixtures of multivariate contaminated normal distributions. *Biometrical Journal*, 58(6):1506–1537.
- Shreeves, P. and Andrews, J. L. (2019). A bootstrap-augmented alternating expectation-conditional maximization algorithm for mixtures of factor analyzers. *Stat*, 8(1):e243.
- Tipping, M. E. and Bishop, C. M. (1999). Mixtures of probabilistic principal component analyzers. *Neural computation*, 11(2):443–482.
- Torres-Carrasquillo, P. A., Reynolds, D. A., and Deller, J. R. (2002). Language identification using gaussian mixture model tokenization. In *2002 IEEE international conference on acoustics, speech, and signal processing*, volume 1, pages I–757. IEEE.

- Vempala, S. and Wang, G. (2004). A spectral algorithm for learning mixture models. *Journal of Computer and System Sciences*, 68(4):841–860.
- Von Luxburg, U. (2007). A tutorial on spectral clustering. *Statistics and computing*, 17(4):395–416.
- Yu, J. (2012). Online quality prediction of nonlinear and non-gaussian chemical processes with shifting dynamics using finite mixture model based gaussian process regression approach. *Chemical engineering science*, 82:22–30.